



HAL
open science

Disease modeling by efficient genome editing using a near PAM-less base editor in vivo

Marion Rosello, Malo Serafini, Luca Mignani, Dario Finazzi, Carine Giovannangeli, Marina C Mione, Jean-Paul Concordet, Filippo del Bene

► To cite this version:

Marion Rosello, Malo Serafini, Luca Mignani, Dario Finazzi, Carine Giovannangeli, et al.. Disease modeling by efficient genome editing using a near PAM-less base editor in vivo. *Nature Communications*, 2022, 13 (1), pp.3435. 10.1038/s41467-022-31172-z . mnhn-03868574v1

HAL Id: mnhn-03868574

<https://mnhn.hal.science/mnhn-03868574v1>

Submitted on 25 Nov 2022 (v1), last revised 9 Dec 2022 (v2)

HAL is a multi-disciplinary open access archive for the deposit and dissemination of scientific research documents, whether they are published or not. The documents may come from teaching and research institutions in France or abroad, or from public or private research centers.

L'archive ouverte pluridisciplinaire **HAL**, est destinée au dépôt et à la diffusion de documents scientifiques de niveau recherche, publiés ou non, émanant des établissements d'enseignement et de recherche français ou étrangers, des laboratoires publics ou privés.

1 **Disease modeling by efficient genome editing using a near**
2 **PAM-less base editor *in vivo*.**

3

4 Marion Rosello¹, Malo Serafini¹, Luca Mignani², Dario Finazzi², Carine Giovannangeli³,
5 Marina C Mione⁴, Jean-Paul Concordet^{3*} and Filippo Del Bene^{1*}

6

7 **Affiliations**

8 ¹Sorbonne Université, INSERM U968, CNRS UMR 7210, Institut de la Vision, Paris,
9 France.

10 ²Department of Molecular and Translational Medicine, University of Brescia, Brescia,
11 Italy

12 ³Muséum National d'Histoire Naturelle, INSERM U1154, CNRS UMR 7196, Paris,
13 France.

14 ⁴Department of Cellular, Computational and Integrative Biology – CIBIO, University of
15 Trento, Trento, Italy.

16

17 **Corresponding authors:**

18 Jean-Paul Concordet*: jean-paul.concordet@mnhn.fr

19 Filippo Del Bene*: filippo.del-bene@inserm.fr

20 **Abstract**

21

22 **Base Editors are emerging as an innovative technology to introduce point**
23 **mutations in complex genomes. So far, the requirement of an NGG Protospacer**
24 **Adjacent Motif (PAM) at a suitable position often limits the editing possibility to**
25 **model human pathological mutations in animals. Here we show that, using the**
26 **CBE4max-SpRY variant recognizing nearly all PAM sequences, we could**
27 **introduce point mutations for the first time in an animal model and achieved up**
28 **to 100% efficiency, thus drastically increasing the base editing possibilities.**
29 **With this near PAM-less base editor we could simultaneously mutate several**
30 **genes and we developed a co-selection method to identify the most edited**
31 **embryos based on a simple visual screening. Finally, we applied our method to**
32 **create a new zebrafish model for melanoma predisposition based on the**
33 **simultaneous base editing of multiple genes. Altogether, our results**
34 **considerably expand the Base Editor application to introduce human disease-**
35 **causing mutations in zebrafish.**

36 **Introduction**

37 The CRISPR (Clustered Regularly Interspaced Short Palindromic Repeats)/Cas9
38 system is a very powerful gene editing tool to perform mutagenesis in zebrafish¹. The
39 sgRNA-Cas9 complex first binds to target DNA through a Protospacer Adjacent Motif
40 (PAM) and Cas9 next cleaves DNA upon stable annealing of the sgRNA spacer
41 sequence to the sequence immediately upstream of the PAM. The NGG PAM
42 sequence is thus required for the *SpCas9* protein to introduce a DNA double-strand
43 break (DSB). This technique is now extensively used in zebrafish to produce knock-
44 out alleles². Additionally, recent studies showed that exogenous DNA and Single
45 Nucleotide Polymorphisms (SNPs) can be introduced in the genome using
46 CRISPR/Cas9 mediated homology-directed (HDR) repair with variable efficiency^{3, 4, 5}.
47 In order to complement these HDR-based strategies to introduce specific point
48 mutation, second generation gene editing tools called base editors (BEs) have recently
49 been developed. The Cytidine Base Editor (CBE) is composed of a Cas9(D10A)
50 nickase fused to a cytidine deaminase and converts C-to-T bases in a restricted
51 window of 13 to 19 nucleotides (nt) upstream of the PAM sequence without inducing
52 double-stranded DNA cleavage^{6, 7, 8}. In zebrafish, several CBE variants have been
53 shown to work with different gene editing efficiencies^{9, 10, 11, 12}. In a previous study we
54 tested several CBE variants and we were able to reach a C-to-T conversion efficacy
55 of 91% in zebrafish, showing many applications from signaling pathway activation to
56 human disease modeling¹². It has been shown that potentially all C bases within the
57 PAM [-19, -13] bp window can be edited with these tools, although a higher efficiency
58 was generally achieved for the Cs located in the middle of this editing window,
59 highlighting the importance of the C distance to the PAM for efficient base editing¹³.
60 Therefore, the restriction of the base modification to the PAM-dependent window is still
61 a critical intrinsic limitation to the base editor techniques. Due to this restriction, these
62 tools cannot be applied to any gene and any mutation of interest. To overcome this
63 limitation, extensive works have been done in cultured cells to engineer CBEs
64 recognizing other PAM sequences than the classical NGG and thereby significantly
65 expand the range of C bases that can be converted. Based on the technological
66 advances made in cultured cells, we tested several novel CBEs in zebrafish to
67 overcome the PAM limitation. Among them, the most recent and flexible variant is the
68 CBE4max-SpRY, reported as a near PAM-less base editor recognizing almost all PAM
69 sequences in cultured cells¹⁴. Here we established the CBE4max-SpRY CBE variant

70 for the first time in an animal model. Using this variant, we were able to perform in
71 zebrafish C-to-T conversions at an unprecedented high efficiency, reaching up to
72 100%. We show that the CBE4max-SpRY converts C bases efficiently using NRN
73 PAMs in zebrafish and that it is possible to mutate several genes using NGN and NAN
74 PAMs at the same time, increasing drastically the base editing possibilities. With a
75 lower efficiency, we also show base editing using NYN PAMs. Based on these results,
76 we developed a co-selection method to phenotypically identify the most edited
77 embryos following the CBE4max-SpRY, by co-targeting the *tyrosinase* or *slc45a2*
78 genes and selecting larvae based on a lack of pigmentation. Finally, using this
79 approach, we could for the first time in zebrafish simultaneously introduce a loss-of-
80 function mutation in a tumor suppressor gene together with a gain-of-function mutation
81 in an endogenous oncogene. We targeted *tp53* tumor suppressor and *nras* oncogene
82 and generated a new zebrafish model with an abnormal melanocyte growth which is
83 an hallmark of melanoma formation susceptibility¹⁵, without over-expressing mutated
84 oncogenes which has been the main strategy used in zebrafish to model cancer so
85 far^{16, 17, 18, 19}.

86 **Results**

87 **Evaluation of several CBE variants recognizing NGN PAM in zebrafish.**

88 Base editing requires the presence of a PAM at 13 to 19 bp downstream of the targeted
89 C base. This limitation is critical and often makes CBEs unable to introduce the desired
90 point mutation in the genome. To overcome this limitation particularly important when
91 trying to model disease causing mutations in animal models, we first tested three
92 different CBE variants recognizing the NGN PAM: xCas9-BE4²⁰, CBE4max-SpG¹⁴ and
93 CBE4max-SpRY¹⁴. First we injected into one-cell stage embryos the *xCas9-BE4*
94 mRNA with the *tp53 Q170** sgRNA, a sgRNA with which we previously got up to 86%
95 of efficiency using BE4-gam¹². No base conversion was detected by Sanger
96 Sequencing of PCR products of the target region. We next analyzed the efficacies of
97 the recent CBE4max-SpG and CBE4max-SpRY variants in zebrafish by injecting into
98 one-cell stage embryos sgRNAs acting upstream of an NGG PAM that we previously
99 found to be efficient with the original CBEs for 5 different loci¹² (Table 1). We
100 sequenced the target regions from 8 single embryos and a pool of 30 embryos for each
101 gene targeted independently by the AncBE4max, the CBE4max-SpG and the
102 CBE4max-SpRY. We detected C-to-T conversion using the CBE4max-SpG only when
103 targeting *cbl* gene for 1 out of 8 single injected embryos whereas we got C-to-T
104 conversions for the 5 loci and for the majority of the injected embryos analyzed with up
105 to 87% of efficiency using CBE4max-SpRY (Table 1). Although working efficiently, the
106 CBE4max-SpRY seems overall to remain less efficient than the classical AncBE4max.
107 The CBE4max-SpRY has been reported as a near PAM-less base editor in cultured
108 cells, with a higher efficacy using NRN PAMs¹⁴. We thus next chose to analyze its
109 flexibility by targeting genes implicated in the formation of pigments in order to have
110 an easy phenotypic read out of the base conversion efficiency.

111

112 **Total base conversion in F0 embryos using the CBE4max-SpRY and a NAN PAM.**

113 In order to explore the efficiency of the near PAM-less CBE variant in zebrafish, we
114 decided to target the *tyrosinase* and *slc45a2* genes, respectively encoding the enzyme
115 catalyzing the production of melanin²¹ and a solute carrier necessary for the production
116 of melanin²². These two genes are thus necessary for pigment formation and mutations
117 in the human genes are found to be linked to oculocutaneous albinism²³. We aimed at
118 introducing a premature STOP codon in these genes in order to have a phenotypical

119 read out of the base conversion efficiency through the visualization of a lack of
120 pigmentation in the larvae. We designed 3 different RNA guides upstream,
121 respectively, of an NGG, NAN and NGN PAM in order to introduce the W273* mutation
122 in Tyrosinase (Fig. 1a) and 2 different RNA guides upstream of a NAN PAM in order
123 to introduce the W123* or R123* mutation in Slc45a2 (Fig. 1b). Upon independent
124 injections of these sgRNAs with the *AncBE4max* mRNA for the NGG sgRNA and the
125 *CBE4max-SpRY* mRNA for the NGG, NAN and NGN sgRNAs, the larvae showed a
126 range of pigmentation defects. We divided these phenotypes in four groups depending
127 on the severity of the pigmentation defects: wild-type like, mildly depigmented, severely
128 depigmented and albino. Representative pictures of 2 days post-fertilization (2 dpf)
129 larvae for each group are illustrated in Fig. 1c.

130 Upon the injection of the *tyr(W273*)* NGG sgRNA and the *AncBE4max* mRNA, we
131 obtained 50% of mildly depigmented larvae with a small proportion of severely affected
132 larvae whereas surprisingly almost 100% of the injected fish with the *CBE4max-SpRY*
133 mRNA were depigmented (Fig. 1d, columns 2 and 3). Next, using the *tyr(W273*)* NAN
134 sgRNA and the *CBE4max-SpRY*, we obtained 100% of injected larvae showing
135 pigmentation defects with almost 50% exhibiting a total lack of pigmentation (Fig. 1d,
136 column 4). Finally, with the NGN PAM sgRNA, 50% of the injected larvae were poorly
137 depigmented, the base editing efficiency reaching only 20% based on Sanger
138 sequencing analyses (Fig. 1d columns 5, 1f C1). Remarkably in the pool of 9 albino
139 larvae from the injection of the *tyr(W273*)* NAN sgRNA and *CBE4max-SpRY* mRNA,
140 we obtained 100% of C-to-T conversion for the C2 (16 bp away from the PAM) and
141 95% for the C1 (15 bp away from the PAM) by Sanger sequencing (Fig. 1f). We did
142 not obtain this C-to-T efficiency neither using the *tyr(W273*)* NGN sgRNA nor the
143 *AncBE4max* with the *tyr(W273*)* NGG sgRNA (Fig. 1d, f). We could speculate that the
144 difference of base conversion efficiency is due to the distance of the C from the PAM
145 or to the sgRNA sequence for which the shift of one DNA base would drastically impact
146 the gene editing efficiency (Fig. 1a). For the mutagenesis of *slc45a2*, we obtained the
147 highest efficiency using the sgRNA designed for generating the W121* mutation using
148 NAN PAM (Fig. 1e). Indeed, upon the injection of the *CBE4max-SpRY* mRNA and the
149 *slc45a2(W121*)* sgRNA, 40% of the larvae were severely depigmented and 19.3%
150 were albinos whereas only mildly depigmented larvae were observed through the
151 injection of the *slc45a2(R123*)* sgRNA (Fig. 1e, f). In order to test if we can use the
152 *CBE4max-SpRY* with NYN PAMs, we designed another sgRNA to introduce the

153 W121* mutation in *Slc45a2* using NTN PAM (Supplementary Fig. 2a). Upon the
154 injection of this sgRNA together with the *CBE4max-SpRY* mRNA, partially
155 depigmented larvae were obtained but no albino and the base editing efficiency
156 reached 55% (Supplementary Fig. 1b, c).

157 Moreover, 4 F0 adult fish mutated for *tyrosinase* and with pigmentation defects were
158 screened and they all transmitted the mutated allele to the offspring with a high
159 transmission rate up to 100% (Supplementary Fig. 2a, b). As for the *tyrosinase*
160 mutants, we screened 7 F0 adult fish injected with the *CBE4max-SpRY* mRNA and the
161 *slc45a2(W121*)* sgRNA. The 5 F0 fish with pigmentation defects transmitted the
162 mutant allele to the offspring (Supplementary Fig. 2a, c) whereas we did not detect the
163 mutant allele in the F1 analyzed embryos from the 2 F0 fish with normal pigmentation.
164 The screening was performed by Sanger sequencing of PCR products of the
165 *tyrosinase* and *slc45a2* regions in random single F1 embryos from an outcross of each
166 founder and no unwanted mutations were identified. We could also observe that the
167 *tyrosinase* Founder 1 and the *slc45a2* Founders 1 and 2 transmitted the mutation to
168 100% of the offspring (Supplementary Fig. 2b, c). Moreover, by crossing 2 founders,
169 *tyrosinase* Founder 1 and 2 in supplementary Fig. 2, we were able to obtain 51.9% of
170 albino larvae (n=28/54) and by crossing the *slc45a2* Founder 1 and Founder 3, 51.1%
171 of the larvae were albinos (n=47/92) (Supplementary Fig. 2d). Together these results
172 highlight the *CBE4max-SpRY* as a very powerful CBE variant, showing that for many
173 targets this CBE could be a better choice than the classical CBEs and could edit 100%
174 of the alleles of the injected embryo using NRN PAMs.

175

176 **Simultaneous base editing of two different genes.**

177 To test if we can take advantage to the high flexibility and efficacy of the *CBE4max-*
178 *SpRY* variant in zebrafish for multiplex base editing, we targeted two loci at the same
179 time using a sgRNA upstream of an NGN PAM and one upstream of a NAN PAM.

180 In order to target the *retinoblastoma1 (rb1)* gene with a higher efficiency than
181 previously using the *rb1(W63*)NGG* sgRNA (Table 1), we designed two sgRNAs, one
182 upstream of an NGN PAM (*rb1(W63*)NGN* sgRNA) and the second upstream of an
183 NAN PAM (*rb1(W63*)NAN* sgRNA) (Fig. 2a). After injection into one-cell stage of each
184 sgRNAs with the *CBE4max-SpRY* mRNA, we sequenced two pools of 9 injected
185 embryos. With both sgRNAs we obtained high base editing efficiency rates, up to 58%
186 of efficiency with the NGN PAM and up to 48% of efficiency with the NAN PAM (Fig.

187 2b). Additionally, we noticed that another C was also edited, leading to the R64K
188 mutation but in 3' to the premature STOP codon introduced (Fig. 2a, b. C3). Using the
189 AncBE4max CBE, this C was at 19 bp from the NGG PAM and the base conversion
190 was not detectable by Sanger sequencing (Table 1) whereas here we show that this
191 C can be converted up to 55% of efficiency (Fig. 2c). This last result shows that for
192 some C base targets, thanks to the PAM flexibility of the CBE4-SpRY, we can now
193 increase the C-to-T conversion efficacy using other sgRNAs compared to the use of
194 the classical AncBE4max (Table 1).

195 We next injected the *CBE4max-SpRY* mRNA and the two synthetic *tyr(W273*) NAN*
196 and *rb1(W63*) NGN* sgRNAs together into the cell at one-cell stage. Among the
197 injected embryos, 100% showed pigmentation defects and at least 50% exhibited total
198 absence of pigmentation (Fig. 2c). It can be noted that this proportion is almost the
199 same as the one obtained after the use of the *tyr(W273*) NAN* sgRNA alone and the
200 *CBE4max-SpRY* mRNA (Fig. 1d, column 4), meaning that the addition of a second
201 guide did not affect the base conversion efficacy at the *tyrosinase* locus. Sequencing
202 of the two loci was performed on the three different pools of larvae separated according
203 to the severity of their pigmentation defects. As expected, the severity of the
204 pigmentation phenotype follows the base conversion efficiency at the *tyrosinase* locus
205 (Fig. 2d). In particular, we found that in the pool of 35 albino larvae, we could no longer
206 detect the wild-type C by Sanger sequencing, suggesting 100% of C-to-T conversion
207 in the *tyrosinase* gene. Remarkably, in the albino pool, up to 44% of C-to-T conversion
208 of the *rb1* gene was detected, revealing that double *tyrosinase* and *rb1* mutations were
209 present in a large proportion of cells (Fig. 2d), while in mildly depigmented zebrafish,
210 base editing of *rb1* was up to 16%. In addition, we found that both mutations were
211 transmitted to the offspring with high transmission rates, as shown by screening the
212 progeny of only one F0 adult fish (Fig. 2e, f). We obtained different combinations of
213 mutations, and we showed that some F1 embryos were mutated for the *tyrosinase*
214 gene alone. At the same time, we noticed that some embryos were mutated for
215 different Cs of the editing windows for each gene (Fig. 2f). With these results we could
216 demonstrate that, using this approach, it is now possible to mutate simultaneously two
217 different genes with high efficiency by combining two different PAM sequences in
218 zebrafish, NAN and NGN PAMs. Additionally, we can observe that the highest
219 efficiency for *rb1* mutation was found in the albino larvae which also have the highest
220 mutation rate for *tyrosinase* as measured by Sanger sequencing.

221

222 **Co-selection strategy to prescreen phenotypically the most edited larvae.**

223 The efficiency of CBE4max-SpRY achieved here above opens the possibility to
224 perform multiplex mutagenesis in zebrafish. Such experiments, however, usually
225 involve time consuming screening to obtain a founder carrying all the desired mutations
226 or long crossing protocols to genetically combine multiple mutations identified in
227 different animals. For this reason, we have decided to take advantage of the high base
228 editing rate of the *tyr*W273*(NAN) and *slc45a2*(W121*) sgRNAs and developed a
229 method for co-selection of base editing to rapidly identify the most edited F0 embryos
230 following CBE4max-SpRY mRNA injections. We first injected the *rb1*(W63*)NGN and
231 *nras* NAN sgRNAs (Fig. 4a) with the near PAM-less CBE4max-SpRY mRNA and found
232 C-to-T conversion rates up to 3% at *rb1* and 50% at *nras* targets in a pool of 50 injected
233 embryos as measured by Sanger sequencing (Fig. 3b). Moreover, at the *nras* locus
234 we can observe that the C base which is at 12 bases away from the PAM has been
235 edited at 23% of efficiency and the C which is at 18 bases away from the PAM has not
236 been edited on the contrary of what we usually observe using the other CBE4 variants
237 (Fig. 3b). From these observations, we can speculate that the editing windows of the
238 CBE4max-SpRY is slightly different than the usual [-19, -13 bp] PAM window and that
239 with the use of this CBE it is possible to target the C bases which are at 12 bases away
240 from the PAM. We then added to the same micro-injection mix the *tyr*(W273*)NAN
241 sgRNA or the *slc45a2*(W121*)NAN sgRNA and obtained larvae showing pigmentation
242 defects that we split in four groups as above (Fig. 1c and Fig. 3c). For each injection,
243 by sequencing the 3 loci in each pool of larvae, we could show that the editing
244 efficiency is higher or lower to the same extent in the 3 targeted loci (Fig. 3d, e). For
245 the co-selection by targeting *tyrosinase*, we could observe by Sanger sequencing
246 analyses that the mildly depigmented larvae were edited up to 41% for *tyr*, 61% for
247 *nras* and no detectable mutation for *rb1* whereas the albino larvae were edited up to
248 95% for *tyr*, 100% for *nras* and 22% for *rb1* (Fig. 3d). For the co-selection by targeting
249 *slc45a2*, the mildly depigmented larvae were edited up to 22% for *slc45a2*, 65% for
250 *nras* and no detectable mutation for *rb1* whereas the severely depigmented larvae
251 were edited up to 62% for *slc45a2*, 98% for *nras* and 15% for *rb1* (Fig. 3e). Base editing
252 co-selection strategies were recently demonstrated in cultured cells²⁴ and have not
253 been reported in animals so far. Using the *tyr*(W273*) NAN or *slc45a2*(W121*) NAN
254 sgRNAs, we show here a powerful strategy to readily obtain the most efficiently C base

255 edited larvae at targeted loci of interest by simply selecting for the less pigmented
256 larvae resulting from co-targeting the genes necessary for the pigmentation.

257

258 **Modeling genetic diseases with combinations of mutations.**

259 We next investigated the ability of CBE4max-SpRY to introduce in zebrafish mutations
260 found in human cancers. The zebrafish has become a powerful *in vivo* model to study
261 a high variety of human cancer types^{16, 17, 18, 19}. However, studies to assess the effects
262 of mutations in oncogenes in the zebrafish model have relied so far on transgenic
263 approaches that express human oncogenes using tissue specific or constitutive
264 promoters. In order to more accurately mimic the impact of cancer somatic mutations
265 that cause the majority of human cancers, we decided to use the CBE4max-SpRY to
266 generate combinations of mutations in endogenous zebrafish genes preserving their
267 normal transcriptional regulation. To test this innovative approach, we aimed at
268 generating an activating mutation in the *nras* gene combined with loss-of-function
269 mutation in the *tp53* tumor suppressor gene. We thus injected into one-cell stage
270 embryos the *CBE4max-SpRY* mRNA, *nras* NAN and *tp53(Q170*)* sgRNAs. We found
271 that 50% of the double injected fish showed an over-all increase of pigmentation at 3
272 dpf (n=36/70), a phenotype never seen upon separate injection of each sgRNA alone
273 nor in the stable *tp53* mutant (REF)(Fig. 4a). To verify that the absence of phenotype
274 when injecting only *nras* NAN sgRNA is not due to a low efficiency of gene editing, we
275 sequenced a pool of 80 injected embryos and we detected high efficiency of base
276 conversion (Fig. 4b). We next randomly selected 4 embryos presenting a pigmentation
277 similar to control embryos and 8 embryos showing an increase of pigmentation after
278 the injection of the sgRNAs targeting *nras* and *tp53* genes. After sequencing both loci,
279 we found indeed a correlation between the hyperpigmentation phenotype and the
280 efficiency of the multi-target approach, as embryos with an increase of pigmentation
281 had more base editing events for *nras* and *tp53* genes than normally pigmented larvae
282 (Fig. 4c). In order to validate the effect of the activating mutation in Nras at the protein
283 level, we checked whether the MAP kinase pathway downstream of Nras signaling is
284 activated by a western blot analysis for phosphorylated ERK1/2¹⁵ (Fig. 4d). We could
285 detect a significant increase of phosphorylated ERK when *nras* is targeted, suggesting
286 an activation of the MAPK cascade downstream of Nras (Fig. 4d, e). We then analyzed
287 the level of expression of several genes downstream of the transcription factor p53:
288 *p21*, *puma* and *baxa* (Fig. 4f). By RT-qPCR analysis, a significant decrease of

289 expression for these 3 genes was observed in larvae when *tp53* was targeted,
290 suggesting successful targeting of p53 (Fig. 4f). Moreover, we observed a significant
291 increase of expression of two anti-apoptotic genes, *bcl2* and *mcl1a*, and for *mdm2*
292 coding for a negative regulator of p53 in larvae in which *nras* and *tp53* were targeted
293 (Fig. 4g). These gene expression changes suggest that the simultaneous mutations in
294 *nras* and *tp53* may prevent apoptosis, allowing cells expressing oncogenic Nras, and
295 depleted of *tp53*, to survive, and perhaps proliferate, upon oncogenic transformation.
296 Although both G12 and G13 amino acids in Nras are found mutated in human
297 developing melanoma, the patients carry a single mutation. We thus aimed at targeting
298 only the G12 in order to get a zebrafish model closer to human genetic events. We
299 designed sgRNAs targeting a locus upstream of NCN PAMs (Supplementary Fig. 2d).
300 Upon independent injections of each sgRNA with the *CBE4max-SpRY* mRNA, we
301 could detect base editing by Sanger sequencing, reaching 82% of efficiency in a single
302 embryo (Supplementary Fig. 2e, f). This proves that we can generate precise base
303 editing using the CBE4max-SpRY and NCN PAM in zebrafish.
304 Moreover, we showed for the first time that simultaneous activation of endogenous
305 *nras* oncogene and knock-out of *tp53* tumor suppressor gene leads to an increase of
306 melanocyte numbers in zebrafish larvae, an early evidence of abnormal melanocyte
307 growth which could lead to melanoma formation (Fig. 4). Indeed, it has been reported
308 that fish over-expressing human mutant HRAS oncogene in melanocytes were
309 hyperpigmented at 3 dpf and developed melanoma at the adult stage¹⁵. Moreover,
310 other reports using zebrafish transgenic lines have suggested a role of p53 and Ras
311 oncogenes in melanoma formation^{25, 26}. We have developed here for the first time a
312 hyper-pigmentation zebrafish model by generating endogenous activating mutation in
313 *nras* oncogene and loss-of-function mutation in *tp53* tumor suppressor gene.

314

315

316

317

318 Discussion

319 While the Base Editor technology is emerging as a revolutionary method to introduce
320 precise single mutation in the genome, the presence of the NGG PAM sequence at
321 the good localization from the targeted base, defining the base editing window, is
322 necessary and often a constrain. This has restricted its potential applications as the
323 absence of the PAM puts the CBE unusable for many targets of interest. Here, we
324 addressed these limitations in zebrafish by testing several base editor variants
325 recognizing other PAM sequences. We unfortunately did not obtain any C-to-T
326 conversions in zebrafish embryos using the previously published xCas9-BE4²⁰ and
327 with a very low efficiency using the CBE4max-SpG¹⁴ (Table 1, Supplementary Fig.).
328 Nevertheless we could introduce point mutations with a remarkable high efficiency rate
329 using the CBE4max-SpRY variant, a recently described near PAM-less CBE variant
330 engineered and validated in cultured cells but never reported working in an animal
331 model so far¹⁴. We thus significantly expand the base conversion possibilities in
332 zebrafish and open the possibility to convert non NGG-targetable C bases which could
333 not be achieved so far. Through our results, we could demonstrate that the CBE4max-
334 SpRY can be extremely efficient, reaching 100% of C-to-T conversion in at least 50%
335 of the injected embryos (Fig. 2d, e, 3b and 4c). We screened 4 F0 fish for the *tyrosinase*
336 mutation and 5 F0 fish for the *slc45a2* mutation that transmitted the correct mutation
337 to the offspring with a high germline transmission rate (Supplementary Fig. 1). These
338 last results are particularly remarkable as this efficiency rate has never been reached
339 previously in zebrafish, even with the use of the classical CBEs recognizing the NGG
340 PAM^{9, 10, 11, 12}. Moreover, for one of our targets the CBE4max-SpRY was even more
341 efficient than the ancBE4max (Fig. 1d). This could be due also to the fact that the
342 CBE4max-SpRY might have a slightly different editing window than the usual PAM [-
343 19, -13 bp] window as we show base editing for the C12 and no conversion for the C18
344 in *nras* targeting (Fig. 4b). These last results and the PAM flexibility of the CBE4max-
345 SpRY allow now to test several sgRNAs for the mutation of interest and play with the
346 C base localization within the editing window to increase the C-to-T conversion efficacy
347 compared to the use of the classical AncBE4max. These properties allow also to
348 exclude other Cs present in the editing window to avoid the generation of other
349 unwanted mutations near the targeted C. We furthermore demonstrated that using
350 NAN and NGN PAMs we were able to precisely and simultaneously perform the Tyr

351 (W273*) and Rb1 (W63*) mutations with high efficiency rates and both mutations were
352 transmitted to the germline (Fig. 2). In this line, we also performed simultaneously 3
353 different and precise mutagenesis using 3 different PAM sequences (Fig. 3). This
354 ability now in zebrafish is extremely useful if several mutations need to be introduced
355 in order to model a human genetic disease such as cancers, especially if some
356 mutations are located on the same chromosome. Different CRISPR co-selection
357 methods have been engineered in *Drosophila*, *C. elegans* and cultured cells in order
358 to phenotypically detect and enrich the cells or animals in which more mutagenesis
359 events are taking place, by adding an sgRNA conferring a phenotypical read-out if the
360 mutagenesis occurred^{27, 28, 29, 30, 31}. Base editing co-selection strategies were recently
361 demonstrated in cultured cells²⁴ but have not been reported in animals so far.
362 Moreover, these time-saving strategies have never been developed in zebrafish. We
363 here developed a co-selection method for base editing in zebrafish to prescreen
364 phenotypically injected embryos based on the detection of pigmentation defects. The
365 method is based on the addition of the *tyr*(W273*) NAN sgRNA or the *slc45a2*(W121*)
366 sgRNA to the micro-injection mix. Importantly mutations in the *tyr* gene seems to be
367 semi-viable whereas the loss-of-function mutation in the *slc45a2* gene do not affect
368 viability and fertility in zebrafish²¹. We indeed have shown in this study that using this
369 strategy we could select the most depigmented embryos which were the most C-to-T
370 converted for *nras* and *rb1* genes (Fig. 3b, c). We also developed a zebrafish model
371 combining activating mutations of *nras* oncogene and knock-out of *tp53* tumor
372 suppressor gene causing an increase of melanocytes (Fig. 4), a clear melanoma
373 predisposing phenotype. Indeed, fish over-expressing human mutated HRAS
374 oncogene in melanocytes were hyperpigmented at 3dpf and developed melanoma at
375 the adult stage¹⁵. We further validate the effects of these mutations at the protein level
376 by western blot and RT-qPCR analyses. The RT-qPCR analyses also showed that pro-
377 apoptotic genes (*baxa* and *puma*) are downregulated and anti-apoptotic genes (*bcl2*
378 and *mcl1a*) are upregulated, suggesting that this combination of mutations may
379 prevent apoptosis (Fig. 4g, f) and allow cancer cell survival and proliferation. Moreover,
380 the upregulation of the *mdm2* gene coding for a negative regulator of p53 could favor
381 the repression of residual p53 activity in the double mutant in addition to the activation
382 of Nras which confer a growth advantage through pERK signaling pathway (Fig. 4).
383

384 Compared to the other existing genome editing technologies, the cytosine base editor
385 approach seems to be the most efficient to perform C:G to T:A conversion and the
386 design of the sgRNA is more straightforward than the pegRNAs and the knock-in DNA
387 templates^{32, 33, 34, 35}. Moreover, although the presence of INDELS has been revealed
388 by the NGS sequencing for several loci, this frequency remains much lower than the
389 one of the expected mutations in contrast to what was reported for prime editing and
390 in some HDR-based knock-in strategies in zebrafish ^{32, 33, 34, 35}. However, the base
391 editor is limited to the type of modifications and the presence of bystander Cs can be
392 problematic as they can be converted as well. This last problem is nevertheless
393 mitigated by our results with CBE4max-SpRY thanks to the high flexibility of sgRNA
394 design that in most cases can be shifted to target only the wanted mutation. Based on
395 our results, we conclude that CBE technology is a more efficient, easier to design and
396 time saving approach to introduce a specific C:G to T:A mutation into the genome and
397 should be considered as an alternative for prime editing and HDR-based knock-in
398 techniques. The high efficiencies of CBE4max-SpRY obtained in this study and the
399 possibility to precisely mutate simultaneously several genes using different PAMs pave
400 the way for future applications in a tissue specific manner and for genetic disease
401 modeling. For example, it could be implemented in the MAZERATI (Modeling
402 Approach in Zebrafish for Rapid Tumor Initiation) system³⁶ in order to rapidly model
403 and study *in vivo* combinations of endogenous mutations occurring in complex
404 multigenic disorders. Finally, the high flexibility and efficiency of our method to induce
405 combination of specific mutations will allow to rapidly create zebrafish cancer models
406 combining the precise set of mutations found in individual patients. In the long term,
407 these models could be used for rapid and patient specific drug screening for advanced
408 personalized medicine^{17, 37}.

409 **Acknowledgements**

410 We thank Panagiotis Antoniou and Annarita Miccio for sharing the *pCAG-CBE4max-*
411 *SpG-P2A-EGFP* and *pCAG-CBE4max-SpRY-P2A-EGFP* plasmids¹⁴. M.R. was
412 supported by the Fondation pour la Recherche Médicale (FRM grant number
413 ECO20170637481) and la Ligue Nationale Contre le Cancer. Work in the Del Bene
414 laboratory was supported by ANR-18-CE16 "iReelAx", UNADEV in partnership with
415 ITMO NNP/AVIESAN (national alliance for life sciences and health) in the framework
416 of research on vision and IHU FOReSIGHT [ANR-18-IAHU-0001] supported by French
417 state funds managed by the Agence Nationale de la Recherche within the
418 Investissements d'Avenir program.

419

420 **Author contributions**

421 M.R. and M.S. did the experimental works and analyzed the results. M.C.M. helped
422 the design of targets, reviewed and edited the manuscript. M.R., J.P.C., F.D.B.
423 conceived the project and wrote the article. J.P.C., F.D.B. co supervised the study.

424

425 **Competing interests statement**

426 The authors declare that they have no conflict of interest.

427

428 **Subjects**

429 Base editors, zebrafish, genome modifications

430 **References**

431 **Uncategorized References**

- 432 1. Sander JD, Joung JK. CRISPR-Cas systems for editing, regulating and targeting genomes.
433 *Nat Biotechnol* **32**, 347-355 (2014).
434
- 435 2. Hwang WY, *et al.* Efficient genome editing in zebrafish using a CRISPR-Cas system. *Nat*
436 *Biotechnol* **31**, 227-229 (2013).
437
- 438 3. Wierson WA, *et al.* Efficient targeted integration directed by short homology in
439 zebrafish and mammalian cells. *Elife* **9**, (2020).
440
- 441 4. Prykhozhij SV, *et al.* Optimized knock-in of point mutations in zebrafish using
442 CRISPR/Cas9. *Nucleic Acids Res* **46**, e102 (2018).
443
- 444 5. Tessadori F, *et al.* Effective CRISPR/Cas9-based nucleotide editing in zebrafish to model
445 human genetic cardiovascular disorders. *Dis Model Mech* **11**, (2018).
446
- 447 6. Komor AC, Kim YB, Packer MS, Zuris JA, Liu DR. Programmable editing of a target base
448 in genomic DNA without double-stranded DNA cleavage. *Nature* **533**, 420-424 (2016).
449
- 450 7. Komor AC, *et al.* Improved base excision repair inhibition and bacteriophage Mu Gam
451 protein yields C:G-to-T:A base editors with higher efficiency and product purity. *Sci Adv*
452 **3**, eaao4774 (2017).
453
- 454 8. Koblan LW, *et al.* Improving cytidine and adenine base editors by expression
455 optimization and ancestral reconstruction. *Nat Biotechnol* **36**, 843-846 (2018).
456
- 457 9. Zhang Y, *et al.* Programmable base editing of zebrafish genome using a modified
458 CRISPR-Cas9 system. *Nat Commun* **8**, 118 (2017).
459
- 460 10. Carrington B, Weinstein RN, Sood R. BE4max and AncBE4max Are Efficient in Germline
461 Conversion of C:G to T:A Base Pairs in Zebrafish. *Cells* **9**, (2020).
462
- 463 11. Zhao Y, Shang D, Ying R, Cheng H, Zhou R. An optimized base editor with efficient C-to-
464 T base editing in zebrafish. *BMC Biol* **18**, 190 (2020).
465
- 466 12. Rosello M, *et al.* Precise base editing for the *in vivo* study of
467 developmental signaling and human pathologies in zebrafish. *bioRxiv*,
468 2020.2012.2012.422520 (2020).
469
- 470 13. Gaudelli NM, *et al.* Programmable base editing of A*T to G*C in genomic DNA without
471 DNA cleavage. *Nature* **551**, 464-471 (2017).
472
- 473 14. Walton RT, Christie KA, Whittaker MN, Kleinstiver BP. Unconstrained genome
474 targeting with near-PAMless engineered CRISPR-Cas9 variants. *Science* **368**, 290-296
475 (2020).
476

- 477 15. Santoriello C, *et al.* Kita driven expression of oncogenic HRAS leads to early onset and
478 highly penetrant melanoma in zebrafish. *PLoS One* **5**, e15170 (2010).
479
- 480 16. Cayuela ML, *et al.* The Zebrafish as an Emerging Model to Study DNA Damage in Aging,
481 Cancer and Other Diseases. *Front Cell Dev Biol* **6**, 178 (2018).
482
- 483 17. Cagan RL, Zon LI, White RM. Modeling Cancer with Flies and Fish. *Dev Cell* **49**, 317-324
484 (2019).
485
- 486 18. Callahan SJ, *et al.* Cancer modeling by Transgene Electroporation in Adult Zebrafish
487 (TEAZ). *Dis Model Mech* **11**, (2018).
488
- 489 19. Casey MJ, Stewart RA. Pediatric Cancer Models in Zebrafish. *Trends Cancer* **6**, 407-418
490 (2020).
491
- 492 20. Hu JH, *et al.* Evolved Cas9 variants with broad PAM compatibility and high DNA
493 specificity. *Nature* **556**, 57-63 (2018).
494
- 495 21. Antinucci P, Hindges R. A crystal-clear zebrafish for in vivo imaging. *Sci Rep* **6**, 29490
496 (2016).
497
- 498 22. Dooley CM, *et al.* Slc45a2 and V-ATPase are regulators of melanosomal pH
499 homeostasis in zebrafish, providing a mechanism for human pigment evolution and
500 disease. *Pigment Cell Melanoma Res* **26**, 205-217 (2013).
501
- 502 23. Ko JM, Yang JA, Jeong SY, Kim HJ. Mutation spectrum of the TYR and SLC45A2 genes in
503 patients with oculocutaneous albinism. *Mol Med Rep* **5**, 943-948 (2012).
504
- 505 24. Li S, *et al.* Universal toxin-based selection for precise genome engineering in human
506 cells. *Nat Commun* **12**, 497 (2021).
507
- 508 25. Yen J, *et al.* The genetic heterogeneity and mutational burden of engineered
509 melanomas in zebrafish models. *Genome Biol* **14**, R113 (2013).
510
- 511 26. Dovey M, White RM, Zon LI. Oncogenic NRAS cooperates with p53 loss to generate
512 melanoma in zebrafish. *Zebrafish* **6**, 397-404 (2009).
513
- 514 27. Ewen-Campen B, Perrimon N. ovo(D) Co-selection: A Method for Enriching
515 CRISPR/Cas9-Edited Alleles in Drosophila. *G3 (Bethesda)* **8**, 2749-2756 (2018).
516
- 517 28. Ge DT, Tipping C, Brodsky MH, Zamore PD. Rapid Screening for CRISPR-Directed Editing
518 of the Drosophila Genome Using white Coconversion. *G3 (Bethesda)* **6**, 3197-3206
519 (2016).
520
- 521 29. Kim H, *et al.* A co-CRISPR strategy for efficient genome editing in *Caenorhabditis*
522 *elegans*. *Genetics* **197**, 1069-1080 (2014).
523

- 524 30. Liao S, Tammaro M, Yan H. Enriching CRISPR-Cas9 targeted cells by co-targeting the
525 HPRT gene. *Nucleic Acids Res* **43**, e134 (2015).
526
- 527 31. Agudelo D, *et al.* Marker-free coselection for CRISPR-driven genome editing in human
528 cells. *Nat Methods* **14**, 615-620 (2017).
529
- 530 32. Petri K, *et al.* CRISPR prime editing with ribonucleoprotein complexes in zebrafish and
531 primary human cells. *Nat Biotechnol* **40**, 189-193 (2022).
532
- 533 33. Anzalone AV, *et al.* Search-and-replace genome editing without double-strand breaks
534 or donor DNA. *Nature* **576**, 149-157 (2019).
535
- 536 34. Bai H, *et al.* CRISPR/Cas9-mediated precise genome modification by a long ssDNA
537 template in zebrafish. *BMC Genomics* **21**, 67 (2020).
538
- 539 35. Albadri S, Del Bene F, Revenu C. Genome editing using CRISPR/Cas9-based knock-in
540 approaches in zebrafish. *Methods* **121-122**, 77-85 (2017).
541
- 542 36. Ablain J, *et al.* Human tumor genomics and zebrafish modeling identify SPRED1 loss as
543 a driver of mucosal melanoma. *Science* **362**, 1055-1060 (2018).
544
- 545 37. Letrado P, de Miguel I, Lamberto I, Diez-Martinez R, Oyarzabal J. Zebrafish: Speeding
546 Up the Cancer Drug Discovery Process. *Cancer Res* **78**, 6048-6058 (2018).
547
- 548 38. Kluesner MG, *et al.* EditR: A Method to Quantify Base Editing from Sanger Sequencing.
549 *CRISPR J* **1**, 239-250 (2018).
550
551

552 **Methods**

553

554 **Fish lines and husbandry**

555 Zebrafish (*Danio rerio*) were maintained at 28 °C on a 14 h light/10 h dark cycle. Fish
556 were housed in the animal facility of our laboratory which was built according to the
557 respective local animal welfare standards. All animal procedures were performed in
558 accordance with French and European Union animal welfare guidelines. Animal
559 handling and experimental procedures were approved by the Committee on ethics of
560 animal experimentation.

561

562 **Molecular cloning**

563 To generate the *pCS2+_CBE4max-SpG* and the *pCS2+_CBE4max-SpRY* plasmids,
564 each *CBE4max-SpG* and *CBE4max-SpRY* sequence has been inserted into *pCS2+*
565 *plasmid* linearized with EcoRI using the Gibson Assembly Cloning Kit (New England
566 Biolabs). The fragment has been amplified using the primers F-5'-
567 TGCAGGATCCCATCGATTTCGGCCACCATGAAACGGACAG -3' and R-5'-
568 TAGAGGCTCGAGAGGCCTTGTCTAGACTTTCTCTTCTTCTTGG -3') from the
569 *pCAG-CBE4max-SpG-P2A-EGFP* plasmid (Addgene plasmid #139998)¹⁴ and from
570 the *pCAG-CBE4max-SpRY-P2A-EGFP* plasmid (Addgene plasmid #139999)¹⁴.

571

572 **mRNAs synthesis**

573 *pCS2+_CBE4max-SpG* plasmid has been used to generate *CBE4max-SpG* mRNA *in*
574 *vitro*. *pCS2+_CBE4max-SpRY* plasmid has been used to generate *CBE4max-SpRY*
575 mRNA *in vitro*. Each plasmid was linearized with NotI restriction enzyme and mRNAs
576 were synthesized by *in vitro* transcription with 1 µL of GTP from the kit added to the
577 mix and lithium chloride precipitation (using the mMESSAGING mMACHINE sp6 Ultra kit
578 #AM1340, Ambion).

579 *pCMV_ancBE4max⁸* (a gift from David Liu _ Addgene plasmid #112094) has been
580 linearized using AvrII restriction enzyme; mRNAs were synthesized by *in vitro*
581 transcription with 1 ml of GTP from the kit added to the mix and lithium chloride
582 precipitation (using the mMESSAGING mMACHINE T7 Ultra kit #AM1345, Ambion).

583

584 **sgRNA design**

585 The sequenceParser.py python script¹² was used to design *tyr* and *slc45a2* sgRNAs.
586 All the synthetic sgRNAs were synthesized by IDT as Alt-R® CRISPR-Cas9 crRNA.
587 Prior injections, 2 µL of the crRNA (100 pmol/µL) and 2 µl of Alt-R® CRISPR-Cas9
588 tracrRNA (100 pmol/µL) from IDT were incubated at 95°C for 5 min, cooled down at
589 room temperature and then kept in ice.

590

591 **Micro-injection**

592 To make the mutagenesis with base editing, a mix of 1 nL of *CBE* mRNA and synthetic
593 sgRNAs was injected into the cell at one-cell stage zebrafish embryos. For the single
594 mutagenesis, the final concentration was 600 ng/µL for *CBE* mRNA and 43 pmol/µL
595 for sgRNA. For the double *rb1* and *tyr* mutations, the final concentration was 600 ng/µL
596 for *CBE* mRNA and 21 pmol/µL for each sgRNAs. For the double *rb1* and *nras*
597 mutations, the final concentration was 600 ng/µL for *CBE* mRNA and 8,6 pmol/µL for
598 *nras* sgRNA and 34,4 pmol/µL for *rb1* sgRNA. For the double *p53* and *nras* mutations,
599 the final concentration was 600 ng/µL for *CBE* mRNA and 8,6 pmol/µL for *nras* sgRNA
600 and 34,4 pmol/µL for *tp53* sgRNA. For the *tyr* or *slc45a2*, *nras* and *rb1* mutations, the
601 final concentration was 600 ng/µL for *CBE* mRNA, 8,6 pmol/µL for *nras* sgRNA and
602 8,6 pmol/µL for *tyr* or *slc45a2* sgRNA and 25,8 pmol/µL for *rb1* sgRNA.

603

604 **Whole-embryos DNA sequencing _ Primer new genes to add**

605 For genomic DNA extraction, embryos were digested for 1 h at 55°C in 0.5 mL lysis
606 buffer (10 mM Tris, pH 8.0, 10 mM NaCl, 10 mM EDTA, and 2% SDS) with proteinase
607 K (0.17 mg/mL, Roche Diagnostics) and inactivated 10 min at 95°C. To sequence and
608 check for frequency of mutations, each target genomic locus was PCR-amplified using
609 Phusion High-Fidelity DNA polymerase (Thermo Scientific). For the *tyr* locus, a PCR
610 was performed with primers Fwd-5'-ATCGGGTGTATCTGCTGTTTTGG-3' and Rev-
611 5'-CCATACCGCCCCTAGAACTAACATT-3'. For the *rb1* locus, the primers used were
612 Fwd-5'-TCTGTCAACTGTTGTTTTCCAGAC-5' and Rev-5'-
613 CAATAAAAAGACAAGCTCCCCACTG-5'. For the *nras* locus, the primers used were
614 Fwd-5'- CCTTTTCTCTTTTTGTCTGGGTG-5' and Rev-5'-
615 CGCAATCTCACGTTAATTGTAGTGT-5'. For the *tp53* locus, the primers used were
616 Fwd-5'- ATATCTTGTCTGTTTTCTCCCTGCT-5' and Rev-5'-
617 GTCCTACAAAAGGCTGTGACATAC-5'. The DNAs have been extracted on an
618 agarose gel and purified (using the PCR clean-up gel extraction kit #740609.50,

619 Macherey-Nagel) and the sanger sequencings have been performed by Eurofins. The
620 sequences were analyzed using ApE software and quantifications of the mutation rates
621 done using editR online software³⁸.

622

623 **qPCR**

624 For gene expression analysis total RNA was extracted from twenty 5dpf larvae in
625 triplicate (for each experimental group: non-injected, *nras* sgRNA, *tp53* sgRNA or
626 NRAS+p53 sgRNAs with *CBE4max-SpRY* mRNA) with TRIzol reagent (Invitrogen).
627 Total RNA was cleaned up using RNeasy Mini Kit (Qiagen) following the
628 manufacturer's instructions and treated twice with DNase I (1 unit/ μ g RNA, Qiagen).
629 The RNA concentration was quantified using nanodrop2000 (Thermo Fisher) and VILO
630 superscript KIT (Thermo Fisher) was used for First-strand cDNA synthesis according
631 to the manufacturer's protocol. qRT-PCR was performed using SMOBio qPCR Syber
632 Green Mix (TQI-201- PCR Biosystem) using a standard amplification protocol. The
633 primers used are the following:

634

635 puma F: GAACACACGGGTTACAAAAGAC

636 puma R: GAAAATTCCCAGAGTCTGTAAGTG

637

638 baxa F: GTGGCGCTTTTCTACTTTGC

639 baxa R: GGAAACTCCGACTGTCTGC

640

641 p21 F: ACCACTAGAGGGCGGAGACT

642 p21 R: CTGGGGTTTTCTCCACTTCA

643

644 mdm2 F: AGCTGATTGGCTTCCAGAAA

645 mdm2 R: GGTAGTGGCAGGAGATGGAA

646

647 mcl1a F: AAAACAAGAGCTGGCATGGG

648 mcl1a R: CCAAAGACCATGACGGACAAC

649

650 bcl2 F: AACGCCTGTGAAGATGAGGA

651 bcl2 R: TGCAGTCTGGGTCATGTGAT

652

653 (housekeeping)
654 rsp11 F: ACAGAAATGCCCCCTTCACTG
655 rsp11 R: GCCTCTTCTCAAAACGGTTG.

656

657 Data analysis was performed with Microsoft Excel and Graphpad Prism. In all cases,
658 each qPCR was performed with triplicate samples and repeated with at least three
659 independent samples. Data are expressed as fold changes compared to controls.

660

661 **Western blot analysis**

662 Western blot analysis was carried out using standard methods. Briefly, 5 dpf larvae
663 (n=20, x 3 biological replicates) of each experimental group (non-injected, *nras* sgRNA,
664 *tp53* sgRNA or NRAS+p53 sgRNAs with *CBE4max-SpRY* mRNA) were lysed on ice
665 with lysis buffer (150 mmol/L NaCl, 50 mmol/L TRIS pH 7.4, 0.25% NP40 (Sigma-
666 Aldrich; 11754599001), 1mM EDTA, 0.1% Triton X100, 0.1% SDS, 0.1 mg/mL
667 Phenylmethylsulfonyl fluoride, protease cocktail inhibitor (Sigma-Aldrich;
668 04693159001), 50 mmol/L NaF and 10 mmol/L Na3O4V. For Western blots, equal
669 protein concentrations were resolved via 12% SDS–PAGE and transferred to Biorad
670 PVDF membranes. Antibodies used: anti-pERK (Cell Signalling Technology, cat. no.
671 9101S, diluted 1:1000), anti-H3 (Abcam, cat. no. 1791, 1:1000) Goat anti-Rabbit IgG
672 (HRP) Abcam, cat. no. 6721 ECL Western Blotting Substrate (GeneTex, Trident fento
673 Western HRP substrate, cat. no. GTX14698) was added before detection with BioRad
674 Chemidoc XRF+. Band intensity of pERK signals was normalized to levels of H3
675 signal, using Biorad Image Lab software.

676

677 **NGSsequencing**

678

679 **Imaging**

680 Embryos were oriented in egg solution with an anesthetic (Tricaine 0,013%). Leica
681 MZ10F was used to image them. Adult fish were imaged using a net and an Iphone
682 xs.

683

684 **Statistics**

685 A non-parametric t-test with the Mann–Whitney correction was applied to determine
686 significance in base editing. The software used was Prism 7 (GraphPad).

687 **Figures Add graph number, p-value etc.**

688

689 **Table1.**

690

691 **Figure 1. Total base conversion in the F0 embryos with CBE4max-SpRY and a**
692 **NAN PAM.**

693 **a.** Targeted genomic sequence of the *tyrosinase* gene and the 3 different sgRNAs
694 used to introduce the W273* mutation. **b.** Targeted genomic sequence of the *slc45a2*
695 gene and the 2 different sgRNAs used to introduce the W121* or R123* mutation. **a, b**
696 For each sgRNA, the targeted Cs are in red and the PAM sequence is in green. **c.**
697 Lateral view of representative 2 days post-fertilization (dpf) embryos showing different
698 severity of pigmentation defects (wild-type like, mildly depigmented, severely
699 depigmented and albino embryos). Scale bar = 100 μ m. **d.** Proportion of the 4 groups
700 based on the pigmentation defects described in Fig. 1c for each injection: the
701 *ancBE4max* mRNA and the *tyr(W273*)NGG* sgRNA (column 2, 19 embryos in total),
702 the *CBE4max-SpRY* mRNA and the *tyr(W273*)NGG* sgRNA (column 3, 74 embryos
703 in total), the *CBE4max-SpRY* mRNA and the *tyr(W273*)NAN* sgRNA (column 4, 28
704 embryos in total), the *CBE4max-SpRY* mRNA and the *tyr(W273*)NGN* sgRNA (column
705 5, 10 embryos in total). **e** Proportion of the 4 groups based on the pigmentation defects
706 described in Fig. 1c for each injection: the *CBE4max-SpRY* mRNA with the
707 *slc45a2(R123*)* sgRNA (column 2, 100 embryos in total) or with the *slc45a2(R121*)*
708 sgRNA (column 3, 126 embryos in total). **f.** C-to-T conversion efficiency for each
709 targeted Cs and each pool of embryos showing pigmentation defects presented in
710 Fig.1d and Fig.1e. The efficiencies have been calculated using EditR software³⁸ and
711 chromatograms from Sanger sequencing of PCR products.

712

713 **Figure 2. Germline transmission of two mutations generated simultaneously**
714 **using NAN and NGN PAMs.**

715 **a.** Targeted genomic sequence of the *rb1* tumor suppressor gene and the 3 different
716 sgRNAs used to introduce the W63* mutation. For each sgRNA, the targeted Cs are
717 in red and the PAM sequence is in green. **b.** C-to-T conversion efficiency for each
718 targeted Cs in 2 pools of 9 embryos injected with *CBE4max-SpRY* mRNA and
719 *rb1(W63*) NGN* or *rb1(W63*) NAN* sgRNAs. **c.** Proportion of the 4 groups based on
720 the pigmentation lack defects described in Fig. 1c for embryos injected with the
721 *CBE4max-SpRY* mRNA, the *tyr(W273*)NAN* and the *rb1(W63*)NGN* sgRNA (column
722 2, 74 embryos in total). **d.** C-to-T conversion efficiency for each targeted Cs and each
723 pool of embryos showing pigmentation defects presented in Fig. 2c for the *tyrosinase*
724 and *rb1* genes. The efficiencies have been calculated using EditR software³⁸ and
725 chromatograms from Sanger sequencing of PCR products. **e.** Lateral view of a 3
726 months F0 fish injected at one-cell stage embryo with the *CBE4max-SpRY* mRNA, the
727 *tyr(W273*)NAN* and the *rb1(W63*)NGN* sgRNAs and showing pigmentation defects.
728 Scale bar = 5 mm. **d.** Sequenced *tyr* and *rb1* loci of 9 F1 single embryos from the
729 founder fish in Fig. 2e. 6 embryos out of 9 were single edited for *tyrosinase* and 3
730 embryos out of 9 were double edited for *tyrosinase* and *rb1*.

731

732 **Figure 3. Base editing co-selection method.**

733 **a.** Targeted genomic sequence of the *nras* oncogene and the sgRNA used to introduce
734 the activating mutation. The targeted Cs are in red and the PAM sequence is in green.

735 **b.** C-to-T conversion efficiency for each targeted Cs in *nras* and *rb1* genes in a pool of
736 50 embryos injected with *CBE4max-SpRY* mRNA and *nras* NAN and *rb1(W63*)* NGN
737 sgRNAs. The efficiencies have been calculated using EditR software³⁸ and
738 chromatograms from Sanger sequencing of PCR products. **c.** Proportion of the 4
739 groups based on the pigmentation defects described in Fig. 1c for the embryos injected
740 with the *CBE4max-SpRY* mRNA, the *tyr(W273*)*NAN, *nras* NAA and *rb1(W63*)*NGN
741 sgRNAs (column 2, 161 embryos in total) and with the *CBE4max-SpRY* mRNA, the
742 *slc45a2(W121*)*, *nras* NAA and *rb1(W63*)*NGN sgRNAs (column 3, 212 embryos in
743 total). **d-e.** C-to-T conversion efficiency for each targeted Cs and each pool of embryos
744 showing pigmentation defects presented in Fig. 1b for the *tyrosinase*, *nras* and *rb1*
745 genes (**d**) and the *slc45a2*, *nras* and *rb1* genes (**e**). The albino embryos are the most
746 edited for the 3 different loci. The efficiencies have been calculated using EditR
747 software³⁸ and chromatograms from Sanger sequencing of PCR products. n.d.= non-
748 detectable edits by Sanger sequencing.

749

750 **Figure 4. Endogenous activation of *nras* oncogene and knock-out of *tp53* tumor**
751 **suppressor gene led to an increase of melanocyte numbers.**

752 **a.** Lateral view of 3 dpf larvae. The injected embryos edited only for *nras* do not present
753 any defects whereas 50% of the injected embryos targeted for *nras* and *tp53* show an
754 increase of pigmentation. Scale bar= 100 μ m. **b.** DNA sequencing chromatogram of
755 the targeted *nras* gene from a pool of 80 injected embryos with the *CBE4max-SpRY*
756 mRNA and the *nras* NAN sgRNA. C-to-T conversion shows 83% of efficiency for the
757 C in position 16, 81% for the C in position 15, 78% for the C in position 13 and 16%
758 for the C in position 12 bp away from the PAM. Numbers in the boxes represent the
759 percentage of each base at that sequence position. In red are highlighted the base
760 substitutions introduced by base editing while the original bases are in blue. The color
761 code of the chromatogram is indicated in the upper left corner (Adenine green,
762 Cytosine blue, Thymine red, Guanine black). The distance from the PAM sequence of
763 the targeted C base is indicated below the chromatogram. The efficiencies have been
764 calculated using EditR software³⁸ and chromatograms from Sanger sequencing of
765 PCR products³⁸. **c.** Box plot showing the base editing efficiency for *nras* and *tp53*
766 genes for the 4 “wt-like” larvae and the 8 larvae with increased pigmentation from
767 Supplementary Fig. 3. Mann–Whitney test. **d.** Western Blot made on 3 dpf control
768 larvae, *nras* targeted larvae, *tp53* targeted larvae or NRAS and p53 targeted larvae
769 using *CBE4max-SpRY* mRNA and antibodies targeting phosphorylated ERK1/2
770 (pERK) and histone 3. **e.** Blox plot showing the relative band intensity of 3 independent
771 western blot. **f-g.** Quantitative real-time PCR of *p21*, *puma*, *baxa* (**f**) and *bcl2*, *mcl1a*,
772 *mdm2* (**g**) expression levels in 3 dpf control larvae, *nras* targeted larvae, *tp53* targeted
773 larvae or NRAS and p53 targeted larvae using *CBE4max-SpRY* mRNA.

774

775 **Supplementary Figure 1. High germline transmission rate.**

776 **a.** Lateral view of a 3 months F0 fish injected at one-cell stage with the *CBE4max-*
777 *SpRY* mRNA and the *tyr(W273*)*NAN or *slc45a2(W121*)* sgRNA and showing
778 pigmentation lack defect. Scale bar = 5 mm. **b.** Sequenced *tyrosinase* locus of F1
779 single embryos randomly chosen from an outcross of each founder. 16 embryos out of
780 16 were edited for *tyrosinase* for the Founder 1, 13 embryos out of 16 for the Founder
781 2, 3 embryos out of 15 for the Founder 3 and 2 embryos out of 16 for the Founder 4.
782 **c.** Sequenced *slc45a2* locus of F1 single embryos randomly chosen from an outcross
783 of each founder. 16 embryos out of 16 were edited for *slc45a2* for the Founder 1 and
784 2, 5 embryos out of 16 for the Founder 3, 3 embryos out of 15 for the Founder 4 and 1

785 embryo out of 13 for the Founder 5. **d.** Lateral view of 3 dpf F1 larvae from the cross
786 of the *slc45a2* Founder 1 and Founder 3. Scale bar=

787

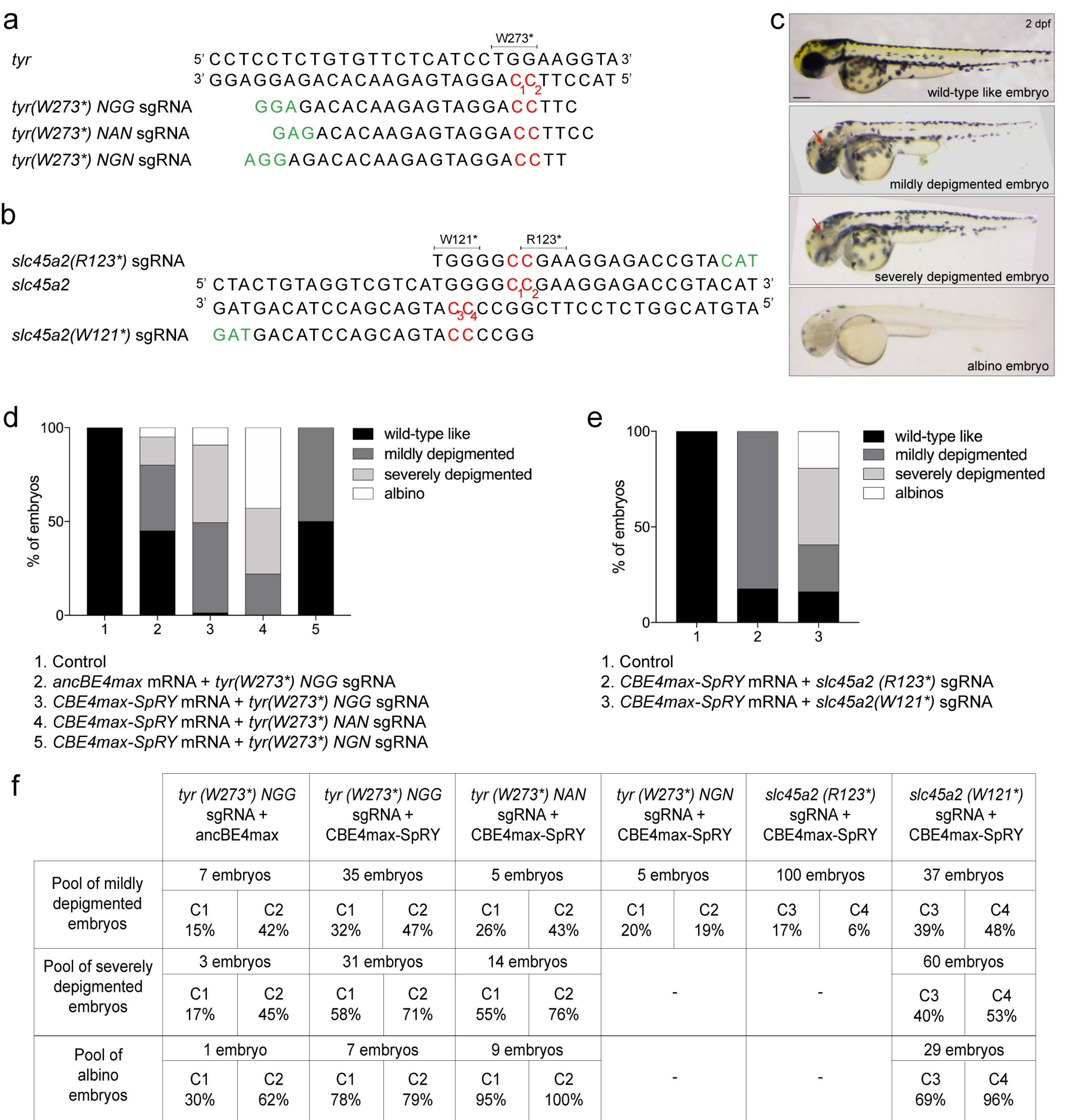
788 **Supplementary Figure 2. CBE4max-SpRY edits NYN PAMs in zebrafish.**

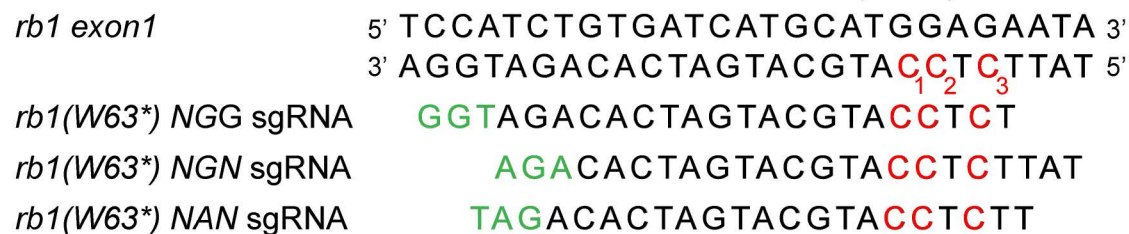
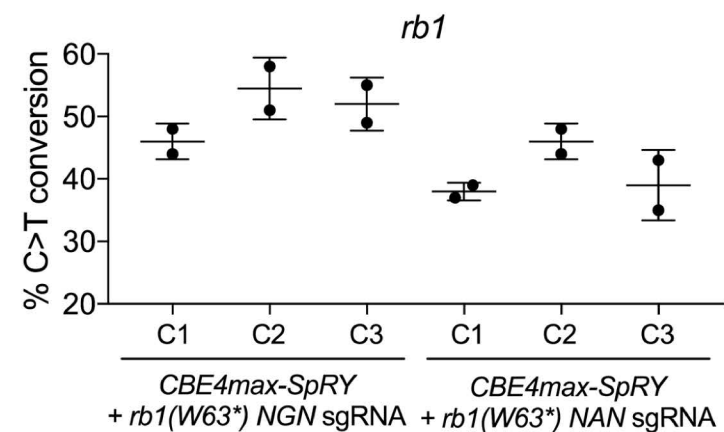
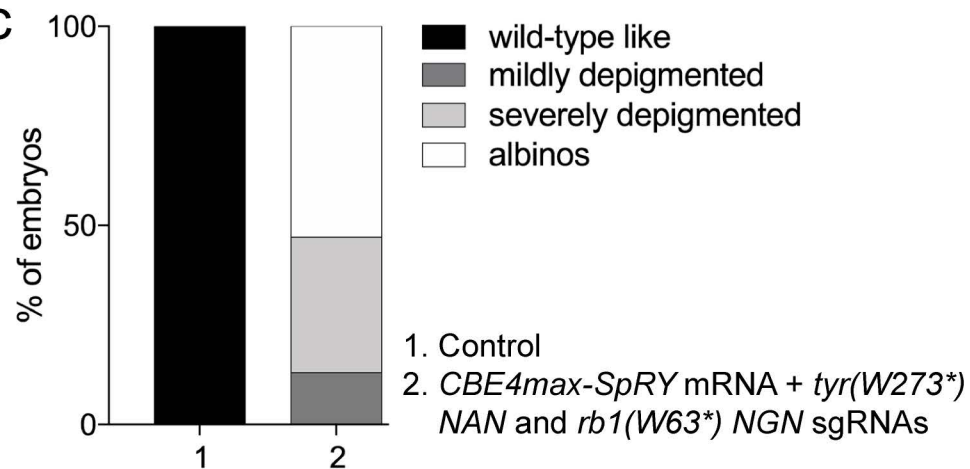
789 **a.** Targeted genomic sequence of the *slc45a2* oncogene and the sgRNAs used to
790 introduce the W121*mutation. The targeted Cs are in red and the PAM sequence is in
791 green. **b.** Proportion of the 4 groups based on the pigmentation lack defects described
792 in Fig. 1c for embryos injected with the *CBE4max-SpRY* mRNA and *slc45a2(W121*)*
793 sgRNA2 (column 2, 108 embryos in total). **c.** C-to-T conversion efficiency for each
794 targeted Cs and each pool of embryos showing pigmentation defects presented in
795 Supplementary Fig. 2b. The efficiencies have been calculated using EditR software³⁸
796 and chromatograms from Sanger sequencing of PCR products. n.d.= non-detectable
797 edits by Sanger sequencing. **d.** Targeted genomic sequence of the *nras* oncogene and
798 the sgRNAs used to introduce the activating mutation. The targeted Cs are in red and
799 the PAM sequence is in green. **e-f.** C-to-T conversion efficiency for each targeted Cs
800 and pool of injected embryos (**e**) or in single embryo randomly selected (**f**) with each
801 sgRNA targeting *nras* and *CBE4max-SpRY* mRNA. The efficiencies have been
802 calculated using EditR software³⁸ and chromatograms from Sanger sequencing of
803 PCR products. n.d.= non-detectable edits by Sanger sequencing.

804

805 **Supplementary Fig. 3.**

806 C-to-T conversion efficiency for each targeted Cs in *nras* and *tp53* genes in single
807 embryos injected with *CBE4max-SpRY* mRNA and *nras NAN* and *tp53 (Q170*)*
808 sgRNAs. 4 single larvae which did not show an increase of pigmentation named as
809 "wt-like" larvae and 8 single larvae showing an increase of pigmentation have been
810 sequenced. n.d.= non-detectable edits by Sanger sequencing.



a**b****c****d**

	<i>CBE4max-SpRY</i> mRNA + <i>tyr</i> (W273*) NAN and <i>rb1</i> (W63*) NGN sgRNAs								
	Pool of 10 mildly depigmented embryos		Pool of 29 severely depigmented embryos			Pool of 35 albino embryos			
<i>tyr</i>	C1	C2	C1	C2	C1	C2	C1	C2	
	32%	52%	51%	67%	95%	100%			
<i>rb1</i>	C1	C2	C3	C1	C2	C3	C1	C2	C3
	16%	14%	13%	16%	21%	16%	35%	44%	39%

e**f**

Mutated sequences found in F1 embryos	number of edited embryo	
	Count	Percentage
<i>tyr</i> CCTTTTAGGATGAGAACACA	1/9	11,1%
<i>tyr</i> CCTTTCAGGATGAGAACACA	5/9	55,6%
<i>tyr</i> CCTTTCAGGATGAGAACACA <i>rb1</i> TATTTTTCATGCATGATCAC	2/9	22,2%
<i>tyr</i> CCTTTTAGGATGAGAACACA <i>rb1</i> TATTTTTCATGCATGATCAC	1/9	11,1%

a

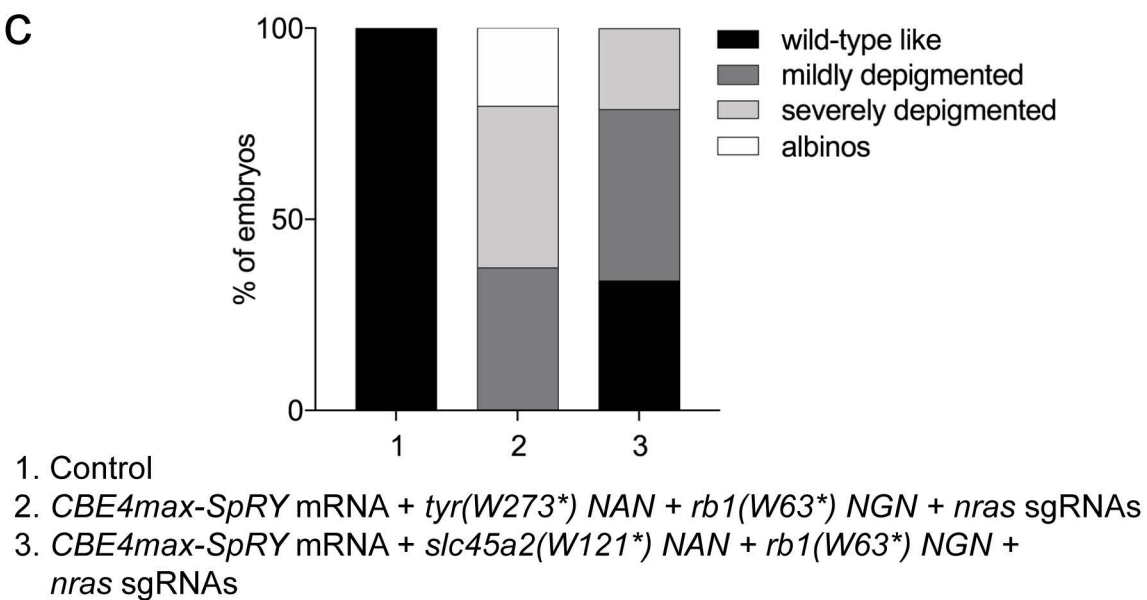


b

Pool of 50 injected embryos:
CBE4max-SpRY mRNA
+ *rb1(W63*) NGN* and
nras NAN sgRNAs

<i>nras</i>	C1	C2	C3	C4
	23%	44%	50%	46%
<i>rb1</i>	C1	C2	C3	
	3%	2%	2%	

c



d

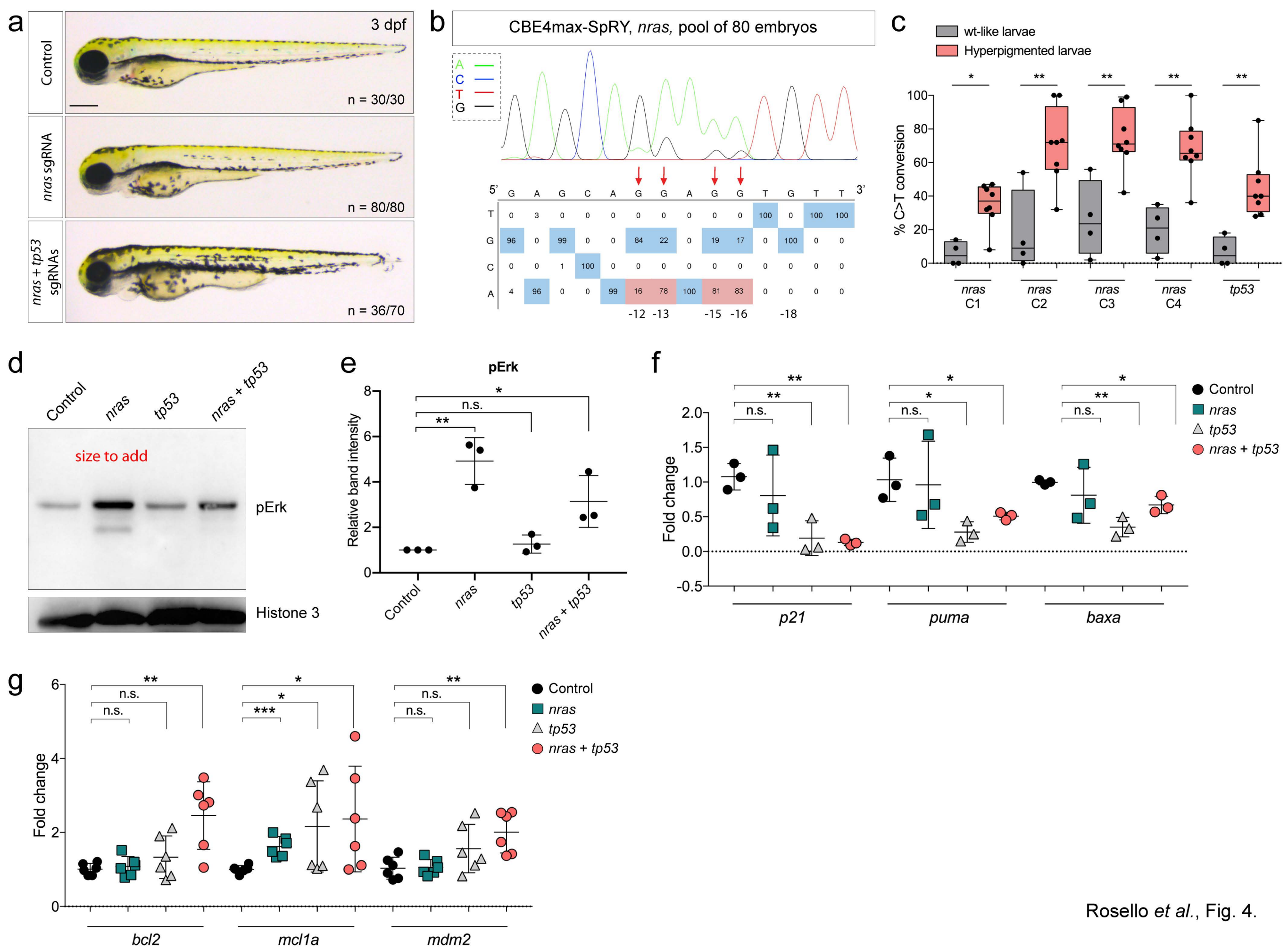
Injected embryos with *CBE4max-SpRY* mRNA
+ *tyr(W273*) NAN*, *rb1(W63*) NGN* and *nras* NAN sgRNAs

	Pool of 60 mildly depigmented embryos				Pool of 68 severely depigmented embryos				Pool of 33 albino embryos			
<i>tyr</i>	C1		C2		C1		C2		C1		C2	
	24%		41%		50%		67%		72%		95%	
<i>nras</i>	C1	C2	C3	C4	C1	C2	C3	C4	C1	C2	C3	C4
	32%	57%	61%	50%	16%	92%	100%	82%	28%	100%	100%	100%
<i>rb1</i>	C1	C2	C3		C1	C2	C3		C1	C2	C3	
	n.d.	n.d.	n.d.		5%	n.d.	n.d.		12%	22%	n.d.	

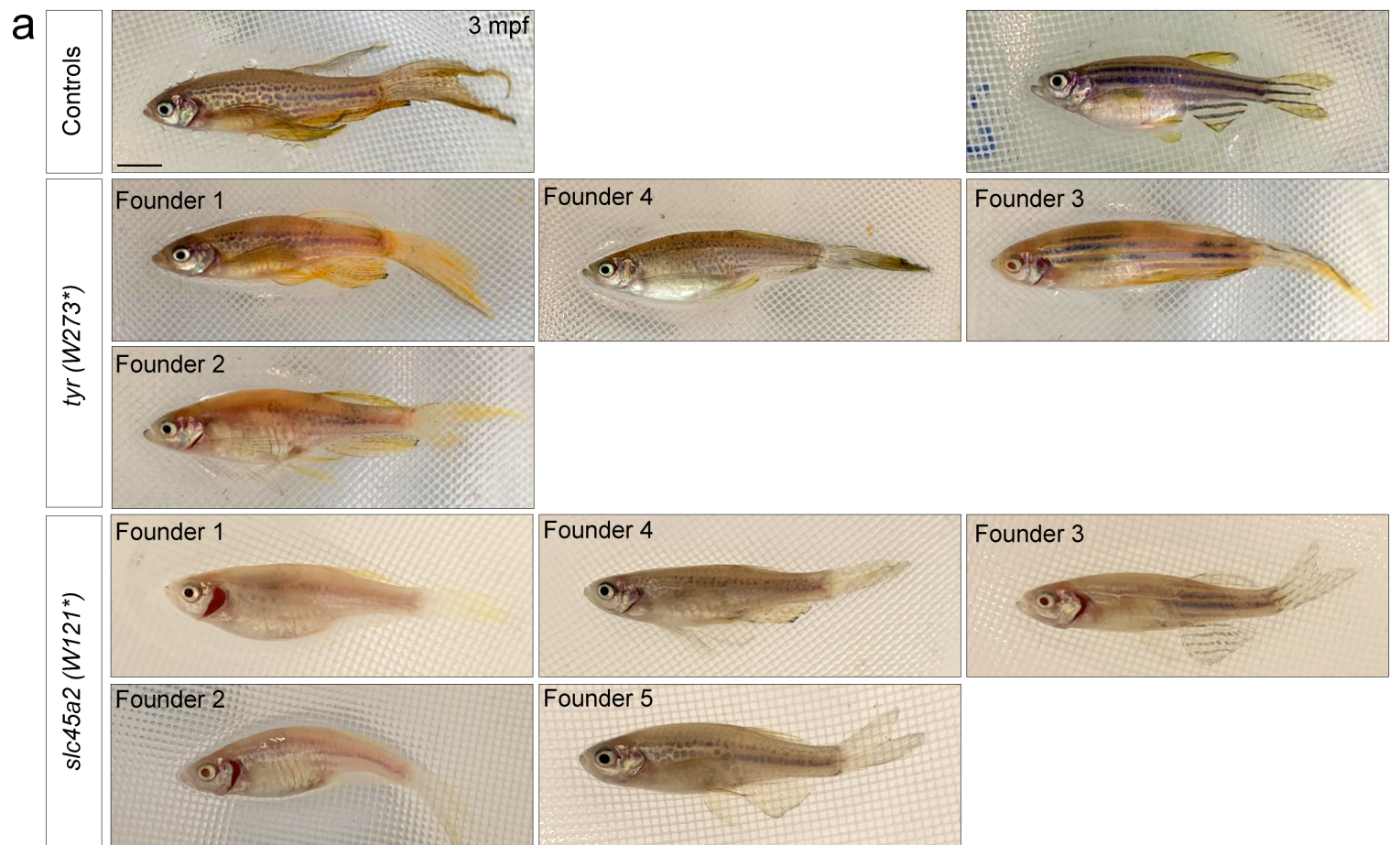
e

Injected embryos with *CBE4max-SpRY* mRNA
+ *slc45a2 (W121*)*, *rb1(W63*) NGN* and *nras* NAN sgRNAs

	Pool of 72 wild-type like embryos				Pool of 95 mildly depigmented embryos				Pool of 45 severely depigmented embryos			
<i>slc45a2</i>	C3		C4		C3		C4		C3		C4	
	n.d.		n.d.		22%		21%		62%		46%	
<i>nras</i>	C1	C2	C3	C4	C1	C2	C3	C4	C1	C2	C3	C4
	n.d.	6%	23%	22%	27%	58%	65%	61%	23%	98%	94%	95%
<i>rb1</i>	C1	C2	C3		C1	C2	C3		C1	C2	C3	
	n.d.	n.d.	n.d.		n.d.	n.d.	n.d.		12%	15%	14%	



	CBE used	number of edited embryos	Emb. 1		Emb. 2		Emb. 3		Emb. 4		Emb. 5		Emb. 6		Emb. 7		Emb. 8		Pool of 30 emb										
<i>bap1</i> (Q173*)	ancBE4max	0/8	n.d.		n.d.																								
	CBE4max-SpG	0/8	n.d.		n.d.																								
	CBE4max-SpRY	6/8	87%		72%		45%		32%		26%		9%		n.d.		n.d.		34%										
<i>tek</i> (Q64*)	ancBE4max	8/8	C14 17%	C13 n.d.	C14 56%	C13 32%	C14 28%	C13 5%	C14 51%	C13 9%	C14 21%	C13 n.d.	C14 26%	C13 19%	C14 51%	C13 22%	C14 29%	C13 n.d.	C14 14%	C13 19%									
	CBE4max-SpG	0/8	C14 n.d.	C13 n.d.	C14 n.d.	C13 n.d.																							
	CBE4max-SpRY	5/8	C14 20%	C13 7%	C14 12%	C13 4%	C14 11%	C13 4%	C14 10%	C13 3%	C14 8%	C13 3%	C14 n.d.	C13 n.d.	C14 n.d.	C13 n.d.	C14 n.d.	C13 n.d.	C14 9%	C13 3%									
<i>cbl</i> (W577*)	ancBE4max	8/8	C16 100%	C15 56%	C16 82%	C15 63%	C16 80%	C15 46%	C16 70%	C15 49%	C16 60%	C15 33%	C16 54%	C15 39%	C16 42%	C15 4%	C16 34%	C15 22%	C16 34%	C15 26%									
	CBE4max-SpG	1/8	C16 9%	C15 8%	C16 n.d.	C15 n.d.	C16 n.d.	C15 n.d.																					
	CBE4max-SpRY	8/8	C16 17%	C15 21%	C16 18%	C15 20%	C16 17%	C15 13%	C16 11%	C15 14%	C16 9%	C15 14%	C16 9%	C15 13%	C16 8%	C15 9%	C16 6%	C15 6%	C16 10%	C15 15%									
<i>dmd</i> (Q8*)	ancBE4max	8/8	15%		27%		12%		13%		19%		9%		12%		8%		15%										
	CBE4max-SpG	0/8	n.d.		n.d.																								
	CBE4max-SpRY	7/8	17%		14%		14%		10%		10%		9%		8%		n.d.		13%										
<i>rb1</i> (W63*)	ancBE4max	5/8	C19 n.d.	C17 n.d.	C16 55%	C19 n.d.	C17 72%	C16 32%	C19 n.d.	C17 44%	C16 7%	C19 n.d.	C17 76%	C16 58%	C19 n.d.	C17 5%	C16 35%	C19 n.d.	C17 n.d.	C16 n.d.	C19 n.d.	C17 n.d.	C16 n.d.	C19 n.d.	C17 n.d.	C16 n.d.	C19 n.d.	C17 37%	C16 16%
	CBE4max-SpG	0/8	C19 n.d.	C17 n.d.	C16 n.d.	C19 n.d.	C17 n.d.	C16 n.d.	C19 n.d.	C17 n.d.	C16 n.d.	C19 n.d.	C17 n.d.	C16 n.d.	C19 n.d.	C17 n.d.	C16 n.d.												
	CBE4max-SpRY	4/4	C19 n.d.	C17 33%	C16 24%	C19 n.d.	C17 22%	C16 n.d.	C19 n.d.	C17 24%	C16 19%	C19 n.d.	C17 31%	C16 24%															

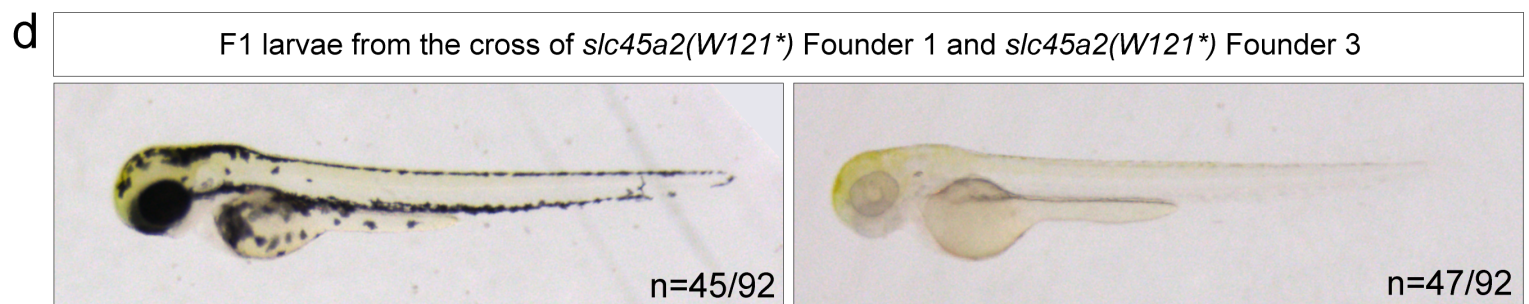


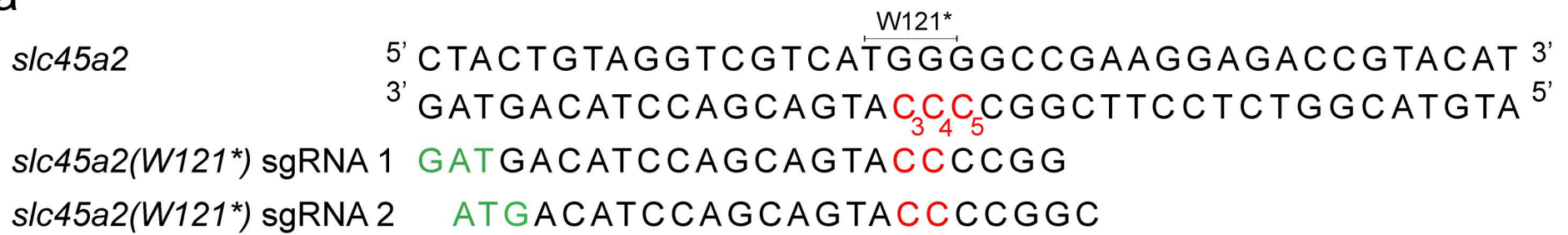
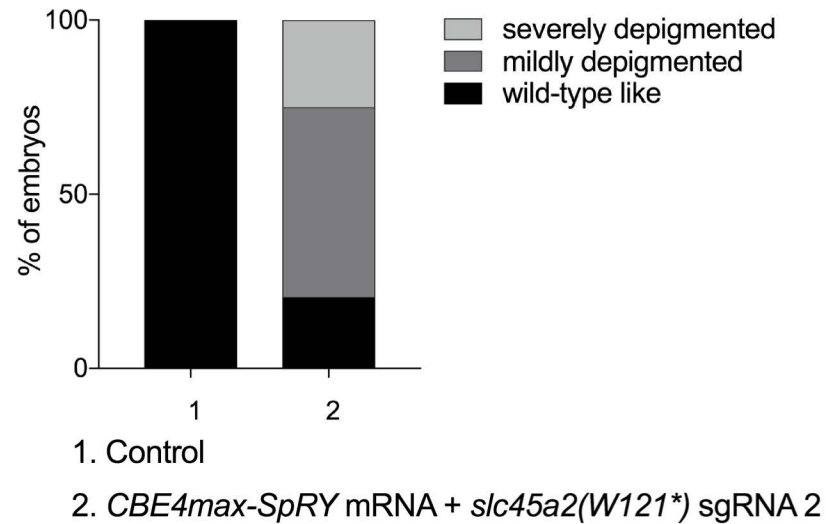
b

<i>tyrosinase</i>	Founder 1		Founder 2		Founder 3		Founder 4	
CCTT CC AGGATGAGAACACA	0/16	0%	3/16	18,7%	12/15	80%	2/16	87,5%
CCTT TT AGGATGAGAACACA	16/16	100%	11/16	68,8%	1/15	6,7%	2/16	12,5%
CCTT TC AGGATGAGAACACA	0/16	0%	2/16	12,5%	2/15	13,3%	0/16	0%

c

<i>slc45a2</i>	Founder 1		Founder 2		Founder 3		Founder 4		Founder 5	
GGCC CC ATGACGACCTACAG	0/16	0%	0/8	0%	11/16	68,7%	12/15	80%	12/13	92,3%
GGCC CT ATGACGACCTACAG	3/16	18,8%	2/8	25%	0/16	0%	2/15	13,3%	1/13	7,7%
GGCC TT ATGACGACCTACAG	13/16	81,2%	6/8	75%	3/16	18,8%	1/15	6,7%	0/13	0%
GGC TTT ATGACGACCTACAG	0/16	0%	0/16	0%	2/16	12,5%	0/15	0%	0/13	0%



a**b****c**

Injected embryos with <i>CBE4max-SpRY</i> mRNA + <i>slc45a2(W121*)</i> sgRNA 2									
	Pool of 22 wild-type like embryos			Pool of 59 mildly depigmented embryos			Pool of 27 severely depigmented embryos		
<i>slc45a2</i>	C3	C4	C5	C3	C4	C5	C3	C4	C5
	n.d.	n.d.	n.d.	30%	32%	21%	53%	55%	33%

d**e**

	Pool of 80 embryos sgRNA 1 (NAN)				Pool of 31 embryos sgRNA 2 (NCN)				Pool of 60 embryos sgRNA 3 (NCN)			
<i>nras</i> CBE4max-SpRY	C1	C2	C3	C4	C1	C2	C3	C4	C1	C2	C3	C4
	16%	78%	81%	83%	8%	12%	n.d.	n.d.	16%	17%	n.d.	n.d.

f

		emb. 1		emb. 2		emb. 3		emb. 4		emb. 5		emb. 6		emb. 7		emb. 8	
<i>CBE4max-SpRY</i>	sgRNA 2	C1	C2	C1	C2	C1	C2	C1	C2	C1	C2	C1	C2	C1	C2	C1	C2
			36%	19%	35%	22%	n.d.	n.d.	n.d.								
<i>CBE4max-SpRY</i>	sgRNA 3	C1	C2	C1	C2	C1	C2	C1	C2	C1	C2	C1	C2	-	-	-	-
			37%	36%	43%	42%	44%	41%	65%	65%	54%	50%	82%	80%			

Larvae injected with <i>CBE4max-SpRY</i> mRNA + <i>nras</i> and <i>tp53</i> sgRNAs	<i>nras</i>				<i>tp53</i>
	C16	C15	C13	C12	C14
“wt-like” larvae 1	27%	29%	6%	n.d.	9%
“wt-like” larvae 2	3%	2%	n.d.	n.d.	n.d.
“wt-like” larvae 3	15%	18%	12%	9%	n.d.
“wt-like” larvae 4	35%	56%	54%	14%	18%
larvae 1 with increased pigmentation	63%	68%	55%	29%	28%
larvae 2 with increased pigmentation	61%	66%	59%	41%	40%
larvae 3 with increased pigmentation	36%	42%	32%	8%	29%
larvae 4 with increased pigmentation	80%	97%	100%	47%	49%
larvae 5 with increased pigmentation	67%	70%	72%	33%	36%
larvae 6 with increased pigmentation	75%	80%	73%	32%	54%
larvae 7 with increased pigmentation	64%	72%	72%	46%	40%
larvae 8 with increased pigmentation	100%	99%	100%	44%	85%